



# Earth's heat flux revised and linked to chemistry

A.M. Hofmeister\*, R.E. Criss

*Department of Earth and Planetary Sciences, Washington University, St. Louis, MO 63130-4899, USA*

Received 20 June 2003; accepted 6 September 2004

Available online 28 October 2004

## Abstract

Recent estimates of the heat flux from the oceanic crust rest on the validity and accuracy of the half-space cooling (HSC) model. The known discrepancies between calculated and measured heat fluxes are not due to hydrothermal circulation, as commonly assumed, because the magmatic source provides too little energy, and the Rayleigh number is too small to foster vigorous convection on an oceanic scale. The half-space cooling model errs in assuming constant thermal conductivity ( $k$ ), but more importantly, provides infinite flux along the ridge centers over all time for any form for  $k$ . This unrealistic global singularity strongly impacts the derived mean flux. We develop three independent methods to ascertain Earth's mean oceanic heat flux directly from compiled heat flow data. The results are congruent, insensitive to uncertainties in the dataset, corroborate previous spherical harmonic analyses, provide the same average flux as from the continents, and constrain the global power as  $31 \pm 1$  TW. Geological observations, inferred mantle overturn rates, estimated mantle cooling rates, and recent geodynamic models independently suggest that neither delayed secular cooling nor primordial heat are currently significant sources, necessitating that current heat production predominately originates in radioactive decay and is quasi-steady-state. Models of Earth's bulk composition based on CI chondritic meteorites provide an unrealistically low radioactive power of  $\sim 20$  TW, whereas enstatite chondrites are sufficiently radioactive to supply the observed heat flux, contain enough iron metal to account for Earth's huge core, and have the same oxygen isotopic ratios as the bulk Earth. We devise a method to obtain K/U/Th ratios for the Earth and other planetary bodies from their power, including secular delays, and use this to constrain Earth's cooling rate. © 2004 Elsevier B.V. All rights reserved.

*Keywords:* Global power; Bulk Earth composition; Cooling mechanisms; Cooling models

## 1. Introduction

The global heat budget (or power,  $Q_{\text{tot}}$ ) is an important constraint for both dynamic and static

models of the Earth. Power is an important input parameter in models of steady-state convection (e.g. [Dubuffet et al., 2002](#)). Moreover, models of planetary evolution and the time dependence of mantle convection require not only  $Q_{\text{tot}}$ , but also knowledge of cooling rates (e.g. [Van den Berg and Yuen, 2002](#)). Thus, quantifying the various heat producing mechanisms is needed.

\* Corresponding author.

*E-mail address:* [Hofmeister@levee.wustl.edu](mailto:Hofmeister@levee.wustl.edu) (A.M. Hofmeister).

Early researchers found good agreement between  $Q_{\text{tot}}$  and radiogenic power ( $Q_{\text{R}}$ ) obtained from chemical models of the Earth based on CI (or C1) meteorites (MacDonald, 1959), giving impetus to such models. Subsequent assessments of Earth's surface heat flux require more heat than compositions based on the CI class can produce. The latest value for  $Q_{\text{tot}}$  of 44 TW (Pollack et al., 1993) is 2.3 times  $Q_{\text{R}}$  provided by various CI models (compiled by Lodders and Fegley, 1998). To explain this difference, additional heat sources and processes have been proposed. Consensus does not exist, and the hypotheses fall into several classes: (i) delayed secular cooling, wherein the surface flux includes stored internal emissions from an earlier age that exceed the current amount generated (see discussions in Van den Berg and Yuen, 2002; Van den Berg et al., 2002), or (ii) high K content in the core (e.g. Breuer and Spohn, 1993), or (iii) remnants of primordial heat ( $Q_{\text{P}}$ ) (e.g. Anderson, 1988a,b) delivered early in Earth's history from impacts of accretion or decay of short-lived isotopes. Other possible heat releasing processes, such as crystallization of the inner core, contribute insignificantly (e.g. Stacey, 1969).

Not all of these hypotheses can be correct. Section 2 reviews geologic observations, estimates of cooling rates, and recent geophysical models, concluding that secular cooling delays are probably below 0.3 Ga, and that other proposals for additional heat can be dismissed. Independent lines of evidence congruently suggest that recent estimates of  $Q_{\text{tot}}$  are too high and that Earth's heat balance currently approximates steady-state conditions. Specifically, Earth's heat loss follows closely the heat production rate (Tozer-type evolution), at least for recent history. Section 3 shows that the mean oceanic heat flux is overestimated due to use of the half-space cooling (HSC) model, and that problems with this model include neglecting the temperature dependence of  $k$ . The value of 44 TW obtained using the HSC model has not been verified by independent means, and conflicts with geochemical and geophysical evidence.

These discrepancies led us to re-examine not only the deduction of  $Q_{\text{tot}}$  from heat flow measurements, but also compositional models of the bulk Earth. We develop three model-independent methods to ascertain mean oceanic flux, plus a diagram that links radiogenic power to composition, taking possible

secular delays into account. This method can be applied to any planetary body, once its surface heat flux is established.

## 2. Background: problems with proposals for heat in excess of radiogenic emissions

As detailed in this section, the three heat sources proposed to account for the discrepancy of surface heat with the C1 model for composition (extreme delays in secular cooling, high K content in the core, or remnants of primordial heat) are not viable. It is thus unnecessary to discuss variants of the above three hypotheses, nor hybrid models. Primordial heat is considered as a distinct category because its time dependence is unknown. Delayed secular cooling is thus discussed in reference to the storage of radiogenic heat from K, U, and Th, and limitations are set on the amount so contributed by combining geologic evidence and thermal models.

### 2.1. Evidence for delays in secular cooling being negligible to modest

The geological record and cooling rates inferred from petrology indicate that delayed cooling, wherein a lag exists between radioactive disintegrations and surface emissions of the associated heat, is unimportant today. Overturn times for the mantle and recent geodynamic models support this conclusion. As detailed below, the available evidence indicates that Earth's current power is mostly that of radiogenic emissions.

Production of oceanic lithosphere via basaltic magmatism for 0.2 to 2 Ga (Burke et al., 1981) suggests quasi-steady-state thermal conditions at present. The rock record is consistent with radioactive heat production being roughly constant over this interval, due to the slow decay rates of extant radioactive isotopes (see Table 10 in Van Schmus, 1995). These slow rates require a delay time exceeding 3 Ga to produce a 44 TW surface flow for the case of negligible current expulsion of accretionary heat and a chondritic composition. Note that for a chondritic composition the power at 3 Ga is 2.3 times the present radioactive heat production (Van Schmus, 1995). A different composition would alter this

relationship in detail, but a twofold increase is roughly correct for the range of K, U, and Th contents that might describe the Earth.

Quasi-steady-state thermal conditions at the present are supported by the low values of time-averaged cooling rates of 30 to 90 K/Ga determined from petrology (Table 2 in Galer and Mezger, 1998). The highest values are derived from komatiite melting temperatures, which may represent atypical Archean hotspots (Abbott et al., 1994; Galer and Mezger, 1998). The best representation for  $\Delta T/\Delta t$  of ~40–50 K/Ga, determined by Abbott et al. (1994) from liquidus temperatures of ancient rock suites, suggests that mantle temperatures from 2.5 to 4 Ga were ~140 to 180 K higher than current temperatures. Assuming this temperature decrease applies to the entire Earth limits the energy loss to 9.4 TW, using the high-temperature heat capacities of perovskite (1 J/g K; Lu et al., 1994) and of Fe alloys (0.5 J/g K). This maximum loss is smaller than the decrease in radiogenic power provided by compositional models of the Earth. For example, a C1 model provides  $Q_R=38$  TW at 3 Ga (the Archean) compared to 19 TW today, see tables and figures in Van Schmus (1995). The decrease in radioactive output more than accounts for the higher temperatures in the Archean, ruling out a significant contribution of any other type of heating to Earth's power.

Large secular delays are also precluded by the known sequestering of radioactive elements into the continental crust, because this layer does not participate in convection, so its release of heat cannot be delayed. Chemical inventories of rocks (summarized by Lodders and Fegley, 1998) indicate that continents carry 8.7 to 16.6 TW. Thus, only the emissions of about half the total radioactive heat derived from a C1 model can possibly be delayed. To account for 44 TW at the surface with a C1 model requires delaying the radioactive emissions of the mantle by 4.2 Ga (see tables in Van Schmus, 1995) which is incompatible with the rock record.

Mantle convection strongly limits retention of heat, as this process is rapid compared to diffusion. An average spreading rate of 3 cm/year means that the whole mantle would overturn in ~0.3 Ga. This small amount of secular delay means that the flux emitted closely follows current radiogenic decay.

Few parameterized convection calculations probe Earth's thermal history. The layered convection model of McKenzie and Richter (1981), which assumes constant viscosity and thermal conductivity, has been used to justify the large secular cooling delay required to reconcile the C1 model with recent estimates of surface flux. In contrast, Tozer (1979) deduced that the strong dependence of viscosity on temperature leads to quasi-steady-state conditions at any given time. The parameterized convection model of Solomatov (2001) that incorporates grain growth, a grain-size dependence for viscosity, and quickly forgotten initial conditions, also provides heat losses that follow the decaying radiogenic isotopes. Recent numerical studies with more realistic parameterizations (Van den Berg and Yuen, 2002; Van den Berg et al., 2002) found that secular cooling delays are limited to 1–2 Ga, even given that a low thermal conductivity ( $k$ ) layer exists and that radiative thermal conductivity is low overall. The recent discovery that radiative transfer in the mantle depends on grain-size and can be large (Hofmeister, 2004a, in review), implies that secular delays are short, and perhaps negligible.

In short, negligible secular delay for the present-day Earth is suggested by the geologic record and plate motions. Recent thermal models are also compatible with quasi-steady-state heat release, given the permissible ranges for the relevant physical parameters.

## 2.2. Limits on the K-content of the core

Estimates for heat production from radioactive elements in the core vary from 0.1 to 8 TW. Low values are associated with experimental and petrological measurements. High values are associated with theoretical arguments, which involve a large number of assumptions.

Iron meteorites, many of which are ascribed to originate in asteroidal cores, have very low amounts of radioactive elements (Mittlefehldt et al., 1998).

Partition coefficients disfavor K enrichment of the core. Measurements at 1 atm set an upper limit on the power of 3.7 TW (Lodders, 1995). High- $T$ , high- $P$  partitioning experiments set more stringent limits of 1.7 TW (Gessmann and Wood, 2002) or 0.4–0.8 TW (Rama Murthy et al., 2003).

One type of theoretical approach involves computing the power across  $D''$ , the boundary layer above the core. Estimates of  $\sim 4$  TW assume a steep gradient across  $D''$  as suggested by the difference between measured melting temperatures for pure Fe at core conditions (Boehler, 2000) and possible mantle geotherms (Anderson, 1988a,b; Hofmeister, 1999). Melting temperatures of an appropriate alloy for the core (e.g. Fe–Ni–S) are not known, and the thermal conductivity of  $D''$  is not well constrained, so these estimates are uncertain.

Other models concern the dynamics or thermal history of the core. One possibility is that the energy powering the dynamo, estimated as 0.1–2 TW (e.g. Gubbins, 1977; Buffett, 2002; Roberts et al., 2003), is equivalent to all heat emissions from the core. Thermal models (e.g. Labrosse, 2003) which assume K contents considerably in excess of those allowed by partitioning experiments suggest high values of 7 TW as the power out of the core. Modeling the core requires using the physical properties of Fe, not core alloys, that are extrapolated from measurements at relatively low  $P$  and  $T$ . For example, the large core power of 8 TW calculated by Anderson (2002) uses

the Weidemann–Franz law to extrapolate  $k$  to core conditions (Stacey and Anderson, 2001). However, neither Fe nor Ni follow the Weidemann–Franz relationship (Sundqvist, 1981, 1982).

Given the associated uncertainties in the above approaches, core power is best constrained by the partitioning experiments listed above. The most recent studies indicate low radiogenic power (0.4–1.7 TW).

### 2.3. Limitations on remnants of primordial heat

The contribution of primordial heat to the current heat budget has been considered to be small (see e.g. Stacey, 1969; Breuer and Spohn, 1993). The arguments made in Section 2.1 against retaining large amounts of radiogenic heat from earlier can also be applied to primordial heat. In addition, release of heat from a finite reservoir diminishes to a nearly constant, low rate at long times (e.g. Carslaw and Jaeger, 1959). Although small amounts of primordial heat may remain today, emission of substantial amounts, as required by the discrepancy of a CI model for composition and a half-space cooling model for the global power, strains credulity.

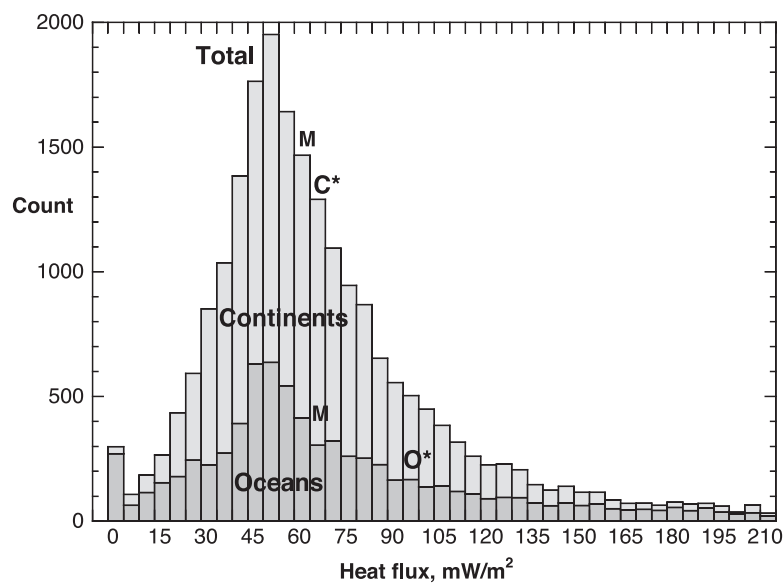


Fig. 1. Histogram of heat flow measurements from the interim compilation (Gosnold and Panda, 2002). The continental data (light grey) are added to the oceanic (medium grey) to produce the total histogram.  $C^*$  is the geologically weighted continental mean and  $O^*$  is the oceanic mean of Pollack et al. (1993) based on the HSC model (Parsons and Sclater, 1977; Stein and Stein, 1992). M indicates median values. Fluxes  $>210$   $\text{mW/m}^2$  are included in the highest bin.

### 3. Re-analysis of global heat flow data

#### 3.1. The average continental heat flux is well-constrained

Pollack et al. (1993) provide the most recent published compilation of surface heat flow measurements. The areal distribution of nine geologic units was used to compute the mean continental flux as 65 mW/m<sup>2</sup> (Table 3 in Pollack et al., 1993), which is higher than the peak at 55 mW/m<sup>2</sup> in the slightly skewed histogram (Fig. 1). Statistical analysis of the interim compilation (Gosnold and Panda, 2002) supports the geologic value. Most continental measurements are from U.S. localities (Fig. 1) which provide most of the fluxes above 200 mW/m<sup>2</sup>. Simple averages (Table 1) computed by excluding either the highest 2.5% of the fluxes or the U.S. subset are consistent with the geologically based mean. The median value of 60 mW/m<sup>2</sup> (Table 1) sets a stringent lower limit, but may represent the true flux because large regions in Africa, South America, the former Soviet Union, and Antarctica remain unprobed (Gosnold and Panda, 2002), and because interesting, high flux localities tend to be over-sampled. Estimates of the continental flux have changed little since 1965, see below, and are thus robust.

#### 3.2. Recent estimates for the average oceanic heat flux are model dependent

In contrast to the continents, the mean oceanic flux has been recently estimated neither from the geographic nor geologic distribution of measurements,

Table 1  
Statistical estimates of heat flux  $J$  in mW/m<sup>2</sup> using the interim compilation (Gosnold and Panda, 2002)

	No. of points	Mean $J$	Median $J$
<i>Continents</i>			
All data ( $J$ up to 4183)	14207	79.7	61
U.S. omitted ( $J < 904$ )	9964	65.8	58
$J < 400$ mW/m <sup>2</sup>	14,089	69	61
$J < 200$ mW/m <sup>2</sup>	13,855	66	60
<i>Oceans</i>			
All data ( $J$ up to 8910)	8272	117.6	64.9
$J < 400$ mW/m <sup>2</sup>	7961	86.2	62.8
$J < 200$ mW/m <sup>2</sup>	7347	70	59

but from the half-space cooling (HSC) model (Parsons and Sclater, 1977; Stein and Stein, 1992; Pollack et al., 1993). In this approach, the measurements at young ages are replaced by calculations using:

$$J = C/t^{1/2} \quad (1)$$

where  $t$  is time and  $C$  is a constant related to the thermal conductivity and other physical parameters. Eq. (1) substantially overestimates the heat flux ( $J$ ) measured from oceanic crust younger than 37 My compared to the measurements (Fig. 2a, also see Pollack et al., 1993; Stein and Stein, 1992). The calculated Quaternary flux exceeds the measurements by 500% (Fig. 2a), leading to 101 mW/m<sup>2</sup> as the mean oceanic value (Pollack et al., 1993), which is almost double the median observed flux of 64.9 mW/m<sup>2</sup> (Table 1). Similar shapes and peak locations of the oceanic and continental histograms (Fig. 1) suggest that using the HSC model forces estimates of the oceanic mean to be too high. The discrepancy between measurements and calculations has been rationalized as due to hydrothermal circulation near the ridge crest (Lister, 1972). However, it can be demonstrated the cause lies elsewhere (Section 3.5). We examine the half-space cooling model from several perspectives, including a probe of the underlying physics.

Model dependence of the estimated mean oceanic flux is evidenced by the historical relationship between the estimates and actual heat flow measurements (Fig. 3). Estimates of the continental flux since 1965 are consistent, and if scaled to represent the whole Earth provide 31–32 TW for the global power, even though the number of data points has increased 10-fold. In contrast, estimates of the oceanic flux initially fluctuate and then markedly increase, and have become increasingly disparate from the growing oceanic database since 1970 (Figs. 2 and 3). Recent values, which are the highest to date, are based on the HSC model.

The half-space cooling model describes some aspects of oceanic heat flux, specifically that as the lithosphere ages, it thickens, cools, and subsides. However, derivation of the global power requires a high degree of accuracy. Insufficient accuracy in the HSC model is indicated by mismatches between both the predicted and measured depths (Fig. 1 in Stein and

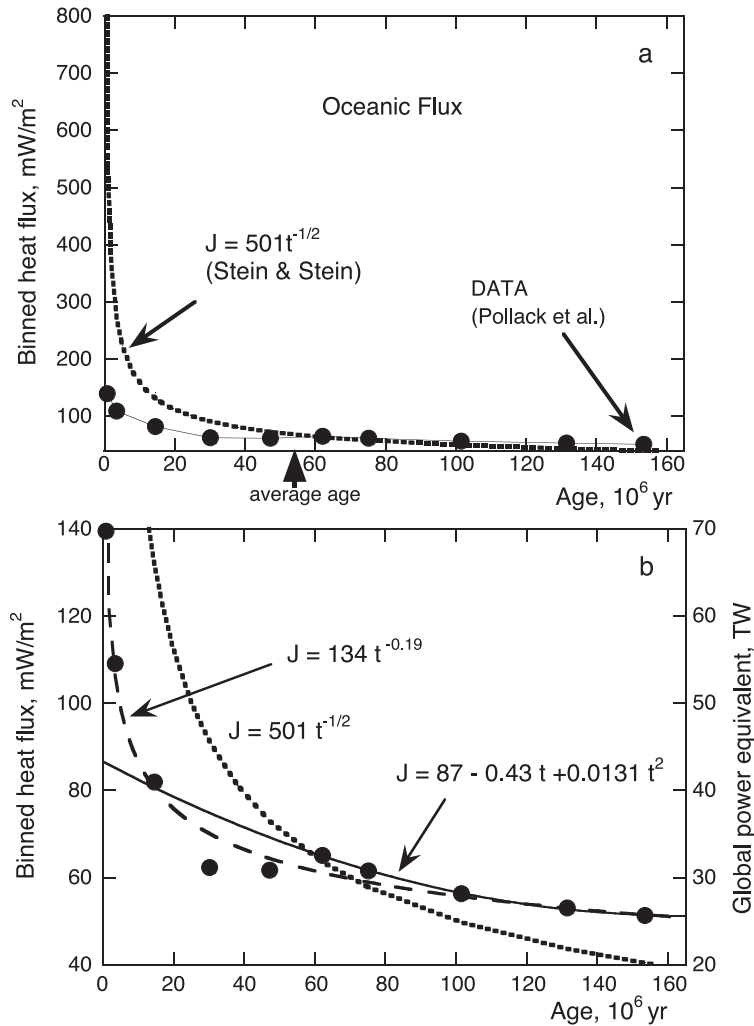


Fig. 2. Oceanic heat flux vs. seafloor age. Data from Table 3 of Pollack et al. (1993). The points are plotted at the mid-point of the time intervals. (a) Comparison of oceanic measurements of heat flux (dots) with the half-space cooling model (Eq. (1), dotted line). Experimental uncertainties in the measured heat flux averaged over these short intervals of time are considerably smaller than the symbols. (b) Various fits to oceanic data. Dotted line=half-space model. Dashed curve=power law fit. Solid line=polynomial fit. Right-axis provides the global equivalent of the power.

Stein, 1992), and between the predicted and measured heat flux (Fig. 2).

The depths are modeled by two equations, depending on whether the age is less than 20 Ma or not. Fig. 1 of Stein and Stein (1992) shows that this model fits the globally averaged, binned depths to 100 Ma, but above this time, the calculated depth curves lie outside the uncertainty of the average. Their Fig. 4 shows that the Northwest Atlantic plate is not fit well at any age and that the North Pacific, African, and South

American plates are not fit well above about ~90 Ma. Notably, heat flow is fit to Eq. (1) with  $C=510 \text{ Ma}^{1/2} \text{ mW/m}^2$  up to 50 Ma, and exponential decay is used thereafter. Eq. (1) does not well describe the data below 50 Ma, yet this is the only part of the HSC model that is used to ascertain mean oceanic flux (Pollack et al., 1993). Above 50 Ma, the heat flux is fit by an exponential decay with time, but the shallow decrease could be modeled by many forms (Fig. 2). Why different cut-off ages were used to fit the depth

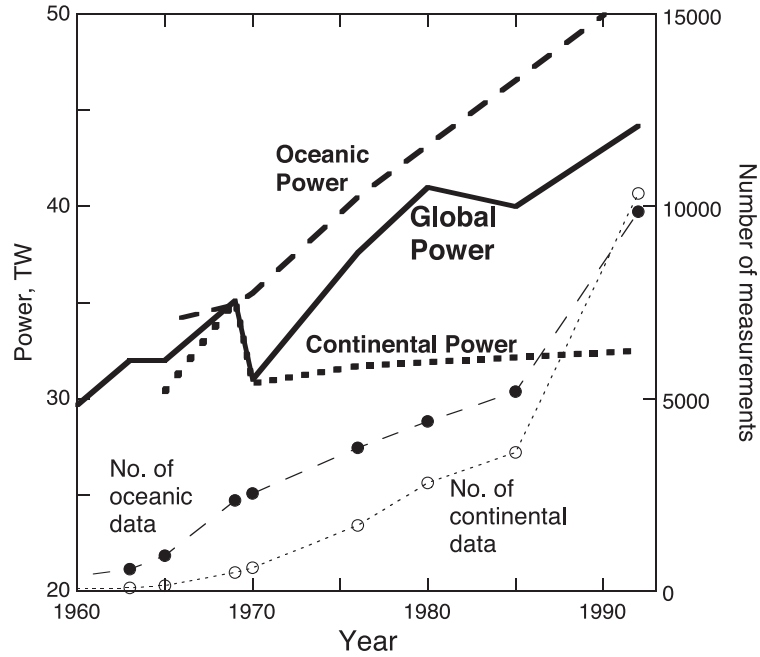


Fig. 3. History of heat flow measurements and estimates of power. Solid line=global power; dashed line=power from oceanic crust, scaled to an Earth-size body; dotted line=continental power, scaled to the whole Earth; all use the left y-axis. Filled circles=number of heat flux measurements from oceanic crust; open circles=continental crust; both use the right y-axis. Data from Lee (1963, 1970); Lee and Uyeda (1965); Horai and Simmons (1969); Jessop et al. (1976); Chapman and Pollack (1980); Chapman and Rybach (1985); Pollack et al. (1993).

and flux data was not addressed. This approach is inconsistent as the equations used for flux and depth were derived from the same model, and the depth and flux constitute a data pair. Apparently, depth and flux

cannot be simultaneously fit by the HSC model and its variants.

The disagreement in depths for the HSC model is generally overlooked, but the misfit in flux for rocks

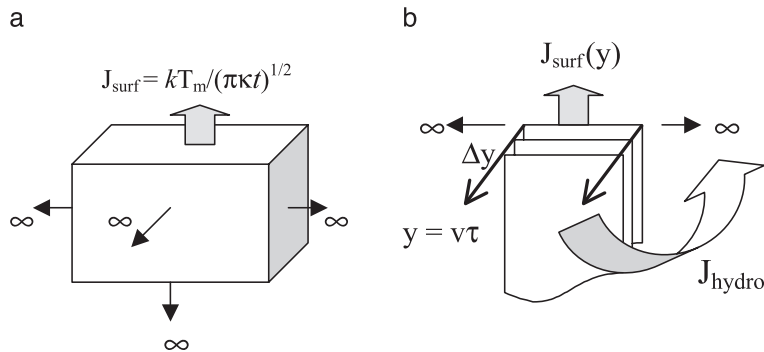


Fig. 4. Comparison of geometries and boundary conditions for the half-space cooling model (a) to that of the spreading plates (b). Note that the model (a) provides a surface flux at a given time. In application to the Earth (b), the surface flux at a place on the ocean plate [ $J(y)$ ] is calculated from the age of the proximal part of the plate. This use converts the time dependent solution to a spatial dependence, and thus, the singularity at  $t=0$  becomes a permanent singularity over arcs on the globe. Geometrically, the oceanic plates (b) are described as a stack of thin slices that are effectively infinite only in  $x$ , not in  $y$ , and thus the equation derived for the infinite half space (a) does not apply. Curved arrow=lateral heat flow of hydrothermal circulation.

having young ages is enormous (Fig. 2a). The 500% difference over the Quaternary has been attributed to advection of ocean water through the oceanic crust with little or no sediment cover (e.g. Pollack et al., 1993), wherein the measured flux is thought to represent the conductive part only, with the fluid being considered to carry a substantial, but unmeasured, portion of the flux. Problems with the hypothesis of hydrothermal circulation are covered in Section 3.5. The half-space cooling model is intended to represent the conductive cooling in the absence of advection, and to give the correct total flux. Through this line of reasoning, the large discrepancy between the HSC model and measurements is rationalized as evidence that the half-space cooling model is needed to determine the true flux, rather than applying spherical harmonic analysis to the actual measurements, as performed by Lee (1970) and others, previous to the development of the HSC model.

Several problems of varying severity are associated with the HSC model. These include the dependence of  $k$  on temperature, the inability of the model to fit the depths and flux simultaneously (Section 3.3), inconsistent input parameters, a singularity in flux at the ridges, and most importantly, the boundary conditions used to derive the equations are inconsistent with the geometry of the ocean plates (Section 3.4).

### 3.3. Systematic errors in the cooling model

The half-space cooling model (Eq. (1)) stems from misapplication of solutions to Fourier's equation in one-dimension:

$$J_c = -k(T, z) dT/dz \quad (2)$$

where  $J_c$  is the conductive portion of the flux,  $k$  is thermal conductivity, and  $z$  is depth. The HSC model presumes that the thermal conductivity is a constant. Whereas the effect of pressure on  $k$  for lithospheric depths is small and can reasonably be neglected, the decrease in  $k$  as temperature increases is strong, and grossly affects the results. The strong dependence is demonstrated in measurements of lavas such as olivine melilites (Buettner et al., 1998), has long been known to exist in minerals found in basalts and mantle rocks (e.g. Slack, 1962; Kanamori et al., 1968; Schatz and Simmons, 1972), and has been addressed theoretically (e.g. Liebfried and Schlömann, 1954;

Hofmeister, 1999, 2004b). The weak pressure dependence is seen in experiments and theory, as summarized by Hofmeister (1999).

The variation of  $k$  with  $T$  grossly impacts conductive models. This is most clearly seen in comparing steady-state solutions to Eq. (2). Assuming constant  $k$  in a steady state model of the half-space provides a linear correlation of temperature ( $T$ ) with depth ( $Z$ ) (Parsons and Sclater, 1977; Stein and Stein, 1992). Accounting for the decrease in temperature dependence of  $k$  in a steady-state model provides the same initial slope, but a much different relationship between  $T$  (in K) and depth  $z$  (in km):

$$T = 277 + 12.297 z + 0.05733 z^2 \quad (3)$$

(Hofmeister, 1999) which becomes increasingly disparate from the constant  $k$  solution as  $z$  increases.

The same sort of discrepancy must exist between the HSC cooling model originated by Parsons and Sclater (1977) which assumes constant  $k$ , and a more realistic time-dependent model, which would include the known rapid decrease of  $k$  as  $T$  increases. It is not necessary to derive an analytical solution to understand the effect. From Eq. (2), it is obvious that the primary consequence of assuming that  $k$  is constant and similar to its ambient value is that the heat flux is overestimated for the hot ridges, which actually have lower  $k$  due to higher temperatures. As the lattice contribution to  $k$  goes as  $\sim 1/T$  to  $\sim 1/T^{1/4}$ , depending on the phase (e.g. Slack, 1962; Kanamori et al., 1968; Schatz and Simmons, 1972; Buettner et al., 1998; Hofmeister, 1999, 2004b), and radiative (Hofmeister, 2004a, in review) and pressure (summarized by Hofmeister, 1999) effects are small in the shallow, oceanic lithosphere, the half-space cooling model can err by a factor of  $\sim 30$ , depending on the specific temperature distribution near the ridge. In essence, incorporating time into the conductive cooling analysis converts the discrepancy in  $T(z)$  found between the steady-state models with constant and variable  $k$  to a systematic error in the heat flux with lithospheric thickness, and thus of heat flux with age.

Fig. 2b shows that Eq. (1), derived for constant  $k$ , does not fit the data well. Better fits are possible for old ages, and even the young ages can be reasonably represented by other simple functions. We also point out that the measured depths for the African plate are

not fit for any ages, and for no plate are the measured depths well represented for ages exceeding 0.1 Ga (see Figs. 1 and 4 in [Stein and Stein, 1992](#)). That the mismatch in depths occurs where the half-space model best describes the heat flux, is another indication that the model is inaccurate.

Thus, the exaggerated estimate of the global flux results from overestimates of heat flux of the ocean floor at young ages from the HSC model ([Fig. 2a](#)), which is due to assuming an unrealistic (constant) thermal conductivity. The temperature at the base of the oceanic lithosphere is also assumed to be constant ([Parsons and Slater, 1977; Stein and Stein, 1992](#)). Assuming a constant basal temperature induces secondary errors, that also contribute to overestimated fluxes at young ages, as the basal temperatures near the ridge of roughly the basalt liquidus are higher than the distant basal temperatures at the basalt solidus or colder.

### 3.4. The singularity at $t=0$ and fundamental shortcomings in plate cooling models

Prediction of infinite flux at  $t=0$  by Eq. (1) indicates that the half-space cooling model is unrealistic. In applying the half-space cooling model to the Earth, time is equated to distance from the ridge ([Fig. 4](#)). Thus, the singularity in time is converted to arcuate singularities that encircle the globe for all time!

That the singularities at the ridge crests impact the mean oceanic flux is demonstrated analytically. The average flux, determined using the HSC model, is:

$$\text{Ave} = \frac{\int_0^{\tau} J(t) dt}{\int_0^{\tau} dt} = \frac{2Ct^{1/2}}{t} \Big|_0^{\tau} = 2J(\tau) \quad (4)$$

Thus, the average flux for crust with ages of 0 to  $\tau$  years is exactly twice the flux observed in the oldest rocks in that interval. Eq. (4) gives a mean oceanic flux of 102.6 mW/m<sup>2</sup> for  $\tau=160$  Ma, the oldest ocean floor. Because the flux for the old seafloor is roughly independent of age, this computation is not influenced by the choice of  $\tau$ . The average predicted by Eq. (4) is equal, within the uncertainty, to the value of  $101 \pm 2$  mW/m<sup>2</sup> obtained by [Pollack et al. \(1993\)](#), which shows that the mean oceanic flux according to the HSC model is thus heavily influenced by the

singularity at  $t=0$ . Obviously, infinite flux is not provided on Earth, no matter how intense the hydrothermal circulation is.

This flaw is independent of the form of  $k(T)$ . Our deduction can be verified by examining the treatment of variable  $k$  by [Carslaw and Jaeger \(1959, Eqs. \(1\)–\(4\) on p. 89\)](#). By representing  $k(T)$  as an integral over temperature, the 1-D equations are recast but the resulting form is unchanged. The singularity is a direct consequence of the assumptions underlying such conductive models.

It is helpful to re-examine the derivation of Eq. (1). Cooling of the semi-infinite plate gives

$$T(t, z) = T_m \text{erf} \left[ z / (4\kappa t)^{1/2} \right] \quad (5)$$

where  $\kappa$  is the diffusivity and  $T_m$  is the basal temperature. The flux obtained from Fourier's equation in one-dimension is proportional to the derivative of Eq. (5):

$$q = -k dT/dz \\ = \left[ k T_m / (\pi \kappa t)^{1/2} \right] \exp \left[ -z^2 / (4\kappa t) \right]. \quad (6)$$

The surface flux is obtained by setting  $z=0$ :

$$q_{\text{surf}} = k T_m / (\pi \kappa t)^{1/2}. \quad (7)$$

The physical parameters in Eq. (7) should all be surface values to be consistent with the derivation. The mean oceanic flux ([Pollack et al., 1993](#)) was computed by fitting the depths to  $k=3.2$  W/m K, determined by averaging over depth, whereas the thermal expansivity used is appropriate for ambient conditions. These values and the particular value of  $T_m$  which fit the depths ([Stein and Stein, 1992](#)) were then used to calculate the flux by [Pollack et al. \(1993\)](#). However, the depths can be fit with other combinations of the parameters  $k$ ,  $\kappa$ , and  $T_m$ , and tradeoffs exist. For example, if  $k=5$  W/m K is used, typical of forsteritic olivine and Mg-rich pyroxenes at ambient conditions ([Horai, 1971](#)), rather than 3.2 W/m K, then the predicted flux is  $\sim 126$  mW/m<sup>2</sup> and  $Q_{\text{tot}} \sim 52$  TW. It is the choice of  $k$  that determines  $Q_{\text{tot}}$  calculated from the HSC model. Because only one of the three fitting parameters  $k$ ,  $\kappa$ , and  $T_m$  can be constrained by fitting the depths to the cooling model, the resulting power is predicated on the choice of the remaining

two parameters. If values for oceanic lithosphere are used to constrain the parameters at ambient conditions, allowing  $T_m$  to vary, then a larger  $Q_{\text{tot}}$ , on the order of 50 TW, would result.

Most importantly, this class of models does not solve the problem of plate motions and cooling (Fig. 4). What the approach truly represents is a solution to Fourier's equation in one-dimension which describes the cooling of a half space defined by a plane at  $z=0$ , extending to  $\pm\infty$  in both the  $x$  and  $y$  directions, wherein the temperature and flux are a function of time and of depth into the plate, and of the plate's thermal properties. This elementary solution is well-known (see Section 2.4 of Carslaw and Jaeger, 1959), and Kelvin's misapplication of it to "prove" that the Earth is less than 100 Ma old is famous. The HSC model involves little more than equating time in Carslaw and Jaeger's equations to the distance from the ridge, which can also be marked in years rather than meters (Fig. 4). Although some treatments of the oceanic plates are more detailed and involve different boundary conditions, only Eq. (1) or Eq. (7) have been used to ascertain the mean oceanic flux. Hence, the singularity at  $t=0$  results from forcing a 1-D infinite plane solution unto the essentially 2-D geometry of the spreading ridges. Further, attributing hydrothermal circulation as the origin of the mismatch between measured and calculated flux, clearly violates the 1-D heat flow of HSC-type models through the requirement of a huge lateral flux (Fig. 4b), and is thus inappropriate justification of the HSC model.

This shortcoming (boundary conditions not being met) is difficult to overcome, suggesting that it is not worthwhile to derive the global power from a more complicated HSC model which accounts for the variation of thermal conductivity and other physical properties with temperature. Alternatives are discussed in Section 4.

### 3.5. Why hydrothermal circulation cannot account for the discrepancy

Hydrothermal circulation cannot cause the huge discrepancy of Fig. 2a because the MOR magmatic system is too small and because hydrothermal systems are weak movers of heat. We summarize theory and data on the MOR and other systems and develop a simple model for the heat flux for a weakly advecting system.

Estimates for the heat fluxes associated with the MOR magmatic systems total only 2 to 4 TW, representing the total energy released every year upon the crystallization and cooling of 15 to 25 km<sup>3</sup> of basaltic magma (e.g. Elderfield and Schultz, 1996). For comparison, about 3 TW of thermal power is predicted to be released in the 1st million years (i.e. near the ridge) according to the HSC model. If *all* the energy produced by the magmatic system were delivered to the surface via hydrothermal convection, the hydrothermal system would only operate for ~1 Ma in a static system, or equivalently would only extend ~1 Ma in the dynamic ridge system. This cooling interval is corroborated by cooling timescales of epizonal intrusions. Of course, much of the heat is removed conductively, and the hydrothermal system around the ridges is considerably smaller than the length scale equivalent to ~1 Ma, and carries considerably less than 3 TW. Neither this duration nor the maximum possible energy of the MOR hydrothermal system is sufficient to explain the far larger difference between heat flow measurements and the HSC model (Fig. 2).

To address this obvious problem, enormous, off-axis hydrothermal convection is called on to account for the large discrepancy between the HSC model and measured data for seafloor with ages of 1 to 65 Ma (e.g. Johnson and Pruis, 2003). First, the huge volumes and short timescales (0.027 Ma) that they suggested for such hypothetical systems are not credible. Most important, the proposed system would operate in the subcritical region where Rayleigh number is only a few percent of the critical number, providing a Nusselt number  $Nu=1$  and essentially conductive heat transport (see below; Triton, 1988). Second, the call for off-axis heat augmentation does not explain the progressively increasing discrepancy between model and measurement as distance from the ridge decreases. Finally, the huge lateral flux envisioned by Johnson and Pruis (2003) violates the conditions needed for the HSC model to be valid (Fig. 4).

Weak hydrothermal circulation near mid-ocean ridges, as indicated by the heat released by the cooling mantle, parallels known behavior of shallow intrusions over large and small scales. Weak circulation in diverse systems has been documented using oxygen isotopic measurements (Norton and Taylor, 1979; Gregory and Taylor, 1981; Criss and Taylor, 1986; Criss and

Champion, 1991; Singleton and Criss, 2004). In essence, near the ridges, the excess heat warms the water in the pore spaces, which is forced to rise by the inward flow of cooler, denser fluid from zones distant to the ridge, in an essentially one-pass system. The weakness of the MOR system is corroborated by turnover timescales of 125 Ma derived from oxygen isotopes (Gregory, 1991), and ~45 Ma from Sr isotopic measurements (Goldstein and Jacobsen, 1987).

The relationship between the Nusselt number,  $Nu$ , and the Rayleigh number provides important constraints as to the effectiveness of heat transport by hydrothermal convection (e.g. Elder, 1981; Triton, 1988). In particular,  $Nu$  quantifies the ratio of total heat flux to the flux that would be delivered by conduction alone. The planforms of hydrothermal systems as mapped by oxygen isotope studies show that fluid circulation is unicellular, i.e. the systems basically are flat Hadley cells that operate below the critical Rayleigh number and have  $Nu=1$  (Triton, 1988; Criss and Hofmeister, 1991). The detailed numerical models of Norton and Knight (1977) confirm this conclusion in that predicted hydrothermal circulation around plutons predominantly occurs as flattened rolls that perturb temperature patterns, yet do not greatly shorten magma cooling times over conductive rates. Oxygen isotope evidence for the convective patterns expected above the critical Rayleigh number has been found on a large scale in only one case, within 1 km of the intrusive stock in the 75 km<sup>2</sup> Comstock Lode hydrothermal system (Singleton and Criss, 2004). Thus, the Rayleigh number is subcritical or barely critical for practically all parts of all systems studied so far, and overall  $Nu \sim 1$ . Low values for  $Ra$  are also estimated for the oceanic crust; for example, Lister (1972) and Sleep and Wolery (1978), respectively, used measured seafloor permeabilities and other properties to estimate that  $Ra$  is 2 times or between 0.1 and 1 times the critical value. The indicted capacity for hydrothermal convection to carry heat in natural systems is thus rather weak, because  $Nu=0.02Ra$  above the critical value for  $Ra$  in porous media (Elder, 1981). Pollack et al.'s (1993) suggestion that fluids are moving heat at 5 times the conductive rate over the entire, Quaternary-aged ocean floor would require high values of  $Ra$  of >5 times the critical value (Elder, 1981); such values cannot be attained on a regional scale with any reasonable input parameters.

Enhancement of near-surface heat flux by advection can be dismissed on the basis of boundary layer theory (see Triton, 1988). The probes used to measure the heat flux are inserted near the surface, where the total flux is essentially conductive. A simple mathematical model verifies this concept, as follows.

The relative contributions of conductive and advective fluxes of heat can be quantified in a simplified, one-dimensional problem featuring steady upward flow of fluid and heat. The total flux  $J_{\text{tot}}$  is the sum of the conductive ( $J_c$ ) and advective ( $J_a$ ) fluxes:

$$J_{\text{tot}} = -k \partial T / \partial z + q C_f T \quad (8)$$

where  $q$  is the fluid flux and  $C_f$  is the heat capacity of the fluid. For respective fixed temperatures  $T_0$  and  $T_L$  at the upper ( $z=0$ ) and lower ( $z=L$ ) levels, the solution is:

$$\frac{T - T_0}{T_L - T_0} = \frac{1 - \exp(-bz)}{1 - \exp(-bL)} \quad (9)$$

where  $b$  is the quantity  $qC_f/k$ . Increasing  $q$  will of course change the temperature profile and will increase the total flux. Nevertheless, at the uppermost levels the entire flux is carried by conduction (Fig. 5), independ-

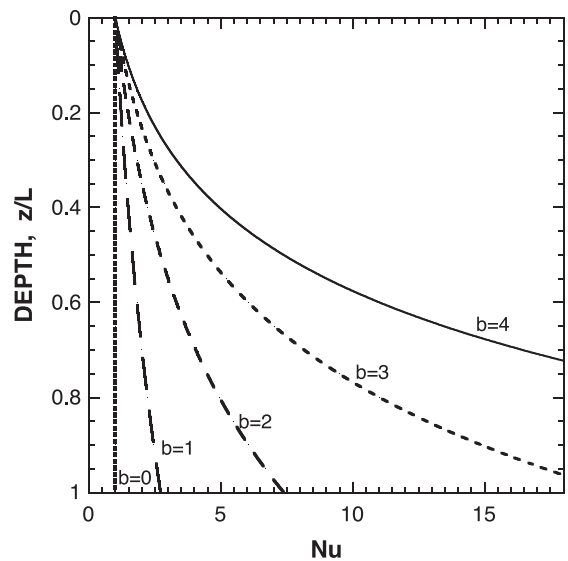


Fig. 5. Relationship between the Nusselt number,  $Nu$ , representing the ratio of the total flux to conductive flux, and the normalized depth  $z/L$  between the cold and hot isothermal levels, for vertical transport of heat and fluid (Eqs. (8) and (9)). At shallower levels the curves all converge to  $Nu=1$ , which is the value for conductive flux. The line  $b=0$  is for no advection.

ent of  $b$ ; the ratio  $J_c/J_{\text{tot}}$  is in fact equal to  $\exp(-bz/L)$  which is unity at  $z=0$ . The probes are inserted in these uppermost levels, and therefore the measured conductive flux is close to the total flux.

In summary, the discrepancy between heat flux measurements and the half-space cooling model has some cause other than hydrothermal circulation. Sections 3.3 and 3.4 show that neglecting the temperature dependence of  $k$ , the singularity at  $t=0$ , and other unrealistic assumptions are the true sources of the discrepancy between calculated and measured heat flux.

#### 4. Alternative methods to establish oceanic heat flux

The mean oceanic heat flux can be extracted from the available data with minimal assumptions. Three independent approaches are used. The first is based on geodynamics, the second approach is geometric, and the third involves numerical integration.

##### 4.1. The mid-cell value of the oceanic flux

We consider the text-book sketch of mid-ocean ridges as overlying the rising portions of the

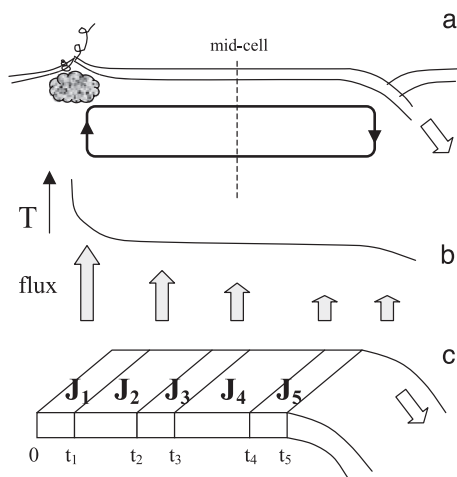


Fig. 6. Schematics used to determine the mean oceanic heat flux. (a) Ocean floor showing ridges, subduction zones, magma, a mantle convection cell, and the mid-cell location. (b) Dependence of the basal lithospheric temperature and mantle heat flux on position in the cell. (c) Conveyor belt model of the ocean floor.

Table 2

Comparison of mean oceanic heat fluxes

Method	Average $J$ , mW/m <sup>2</sup>	Source
C1 Earth	38 <sup>a</sup>	MacDonald (1959)
EH Earth	62 <sup>a</sup>	e.g. Javoy (1995)
Spherical harmonics	62	Lee (1970)
Conveyor belt	62	this work
Mid-cell value	63	this work
Numerical integration	63	this work
Half-space cooling	101	Pollack et al. (1993) <sup>b</sup>

<sup>a</sup> Assumes oceanic and continental fluxes are the same.

<sup>b</sup> Assumes  $k=3.2$  W/m K, rather than  $k_0=5$  W/m K.

convection cells under the oceans, whereas the subducting slabs mark the descending part. In this view, the ridges are hotter primarily because these overlie upwellings in the upper mantle (Fig. 6a). Computational studies of mantle convection (e.g. Van den Berg et al., 2001) portray the average flux and temperature using mid-cell values, thereby avoiding the edge effects which occur in any convecting system (e.g. Triton, 1988). Therefore, the middle of the oceanic cell should emit the mean heat flux (Fig. 6a). The mid-cell region most likely corresponds with the average age of the ocean, ~55 million years (U.S.G.S., 2002). This region is sufficiently distant from the ridges that hydrothermal advection is not expected to have an effect. From Pollack et al. (1993), the average flux of Paleocene (55–65 My) ocean floor is 65.1 mW/m<sup>2</sup>, which resembles fluxes of 61–62 mW/m<sup>2</sup> for both Oligocene–Eocene (25–55 My) and Late Cretaceous floor (65–90 my old). The alternative mid-cell position at ages half of the maximum age of 180 My for the ocean floor (Late Cretaceous) gives a similar value. The resulting mean oceanic flux of 61–65 mW/m<sup>2</sup> is independent of the specifics of convection because the heat flux is similar for any region that could possibly constitute the mid-cell (Table 2, Figs. 2 and 6).

##### 4.2. A conveyor belt model of the ocean floor

Alternatively, we treat the ocean floor as a conveyor belt (Fig. 6c). This model does not depend on any particular linkage of mantle convection with plate motions. Each strip, covering a given span of time,  $\Delta t=t_i-t_{i-1}$ , has an associated mean heat flux,  $J_{\text{mean}}(i)$ . Because the strips are joined over large sections of the globe, and because the production and

motion of the ocean floor occurs at a fairly constant rate overall, the mean ocean heat flux is

$$J_{\text{oceans}} = \frac{1}{t_n} \sum_{i=1}^n (t_i - t_{i-1}) J_{\text{mean}}(i) \quad (10)$$

where  $t_0=0$ . Applying Eq. (10) to the raw data tabulated by Pollack et al. (1993) gives 62.3 mW/m<sup>2</sup>. Omitting the oldest (Jurassic) strip, as such great ages do not occur in all oceans, gives 63.7 mW/m<sup>2</sup>. Omitting the two oldest strips with ages >119 Ma gives 66.0 mW/m<sup>2</sup>.

Hydrothermal circulation has no effect on this calculation as the areas with enhanced and reduced flux average out for such weakly convecting systems. The age distribution of oceanic flow has little effect, as seen by the small change induced by omitting a significant fraction of the old ages (28%). A more precise value might be obtained by performing the sum of Eq. (10) over each known conveyor belt (e.g. the North Atlantic), and then by computing a weighted average based on the areal coverage of each belt, but given the good agreement with the mid-cell value, this level of detail is not needed.

#### 4.3. Numerical integration

Numerically integrating over the binned data in Fig. 2 gives a mean oceanic flux of 63 mW/m<sup>2</sup>. This approach is valid, as the same results were obtained whether Eq. (1) was integrated (Section 3.4) or whether spherical harmonic analysis was applied to the half-space cooling model (Pollack et al., 1993). We tested for sensitivity and found scant difference arises from use of different extrapolations for the endpoints.

#### 4.4. The global power

Our three approaches provide congruent values of the mean oceanic heat flux, Table 2. Our results are independent of any parameterized cooling or tectonic models, and are equivalent to the approach used for the continental data, which suggests the results are robust. Within the uncertainty of the measurements, the mean heat flux of the oceans matches that of the continents, and  $Q_{\text{tot}}$  is  $31 \pm 1$  TW. That oceanic and continental heat fluxes are similar was formerly

accepted (e.g. Lee, 1970). In essence, the most efficient configuration for heat removal occurs when the radioactive rich, but thermally insulating, continents overlie the upper mantle downwellings.

Our result is supported by spherical harmonic analyses of heat flux data which predate the HSC model, all of which provided global powers near 30 TW (Fig. 3). For example, Lee (1970) obtained 31 TW for the global flux from averaging the prior database of 3500 points, of which 2530 were oceanic measurements. The spherical harmonic analysis, like the conveyor belt model, removes any possible effect of weak hydrothermal circulation through averaging. Incorporating the data subsequent to 1970 in a spherical harmonic model will not change the results significantly, because the previous and current histograms are similar, the main difference being extension of the high flux tail. As these extreme fluxes originate from mid-ocean ridges, which constitute a small areal portion of the oceanic crust, the mean is not impacted. Thus, four different approaches to the oceanic flux, all of which are independent of each other and of a cooling model, all return the same mean oceanic flux, and the same global power.

### 5. Links to Earth's bulk composition

Knowledge of Earth's composition is an important constraint for geophysical models. Any viable geochemical model of the bulk Earth must account for the surface heat flux and the oxygen isotope character, and must provide enough Fe for the massive core. These are the observed, first-order features of the Earth. In addition, allowance should be made for secular delays of 0 to 1 Ga.

Rock samples cannot be used reliably because these originate at shallow depths (above about 670 km out of 6370 km, see Gasparik, 2000) with rarity increasing with depth. In addition, mantle samples are distributed unevenly over the globe, and probably reach the surface only under special circumstances (diamond-forming regions are over-represented, for instance). Mineralogical models of the lower mantle (depths >670 km) are poorly constrained as only two parameters, shear and compressional velocities, are observed, whereas the number of variables are many: temperature, mineralogy, and the concentration of

each major element in each mineral present in the various layers at depth. A key parameter used in the comparison, the pressure derivative of the bulk modulus, is virtually identical for all mantle candidate minerals (Hofmeister and Mao, 2003), which increases the uncertainty of determining the mineral phase. Indeed, modeling the unusual velocity gradient in the transition zone with both temperature and pressure derivatives of bulk and shear modulus suggests a gradation in chemical composition (Sino-geikin and Bass, 2002). Estimates of the chemical composition for mantle reservoirs and of the bulk Earth (e.g. Drake and Righter, 2002) thus are predicated on the assumptions, for example, that the lower mantle is chemically homogeneous and similar to the upper mantle. The complex processing that occurred prior to, during, and after accretion and differentiation limits the validity of any detailed chemical model.

The CI model is the longest standing. Even with down-sizing Earth's heat budget from 44 to 31 TW, large  $Q_P$  of 12 TW is still required for a CI model. A secular delay of 1 Ga is equivalent to 5 TW for a CI model (see tables in Van Schmus, 1995). Although such a delay reduces  $Q_P$  to 7 TW, this amount is too large to reconcile with the longevity of basaltic volcanism and inferred mantle cooling rates (Section 2.1). Furthermore, chemical inventories of crustal rocks indicate that continents carry 8.7 to 16.6 TW (summarized by Lodders and Fegley, 1998), leaving mantle convection in such a scenario to be driven almost entirely by delayed or primordial heat. Because  $Q_P$  should be small, alternatives to CI models for Earth's bulk composition must be considered.

First, we assume that  $Q_{\text{tot}}=Q_R$ . As discussed in Section 2.1, low secular delays of 0.3 Ga, expected from geologic observations and mantle overturn rates, provide sufficiently small change in radioactivity that using  $Q_R$  is a good representation of the Earth. In virtually all terrestrial and extraterrestrial rocks (Faure, 1986), Th and U occur close to the average ratio of about 3.75:1. Because this ratio is consistent and K, U, and Th now dominate heat-production,  $Q_R$  for a body of a given size is related to composition by contours on a plot of K vs. U (Fig. 6). We model the bulk silicate Earth (BSE) separately from the metal-rich regions because radioactivity in the core is low, as discussed above, and compare it to the silicate

components of EH meteorites and the Moon (Fig. 7). Typically, EH chondrites contain 40–60 wt.% nearly pure enstatite, 19–28 wt.%  $(\text{Fe,Ni})^0$ , 7–15 wt.% FeS, 5–10% albite, minor silica, and 1 wt.% assorted sulfides, phosphides and nitrides (Rubin, 1997; Brearly and Jones, 1998). The compositions and proportions of the major phases in these meteorites are both simple and consistent (Mason, 1966a; Rubin, 1997; Brearly and Jones, 1998).

From Fig. 7, the bulk silicate Earth can be represented by a simple mixture of lunar (Taylor, 1982; Anders, 1977; Jolliff et al., 2000) and EH materials. All compositions along this line share Earth's oxygen isotopic ratio (Clayton, 1993) and provide 31 TW of radiogenic power. It is thus unnecessary to call on heat sources other than radioactivity to explain Earth's current heat flux.

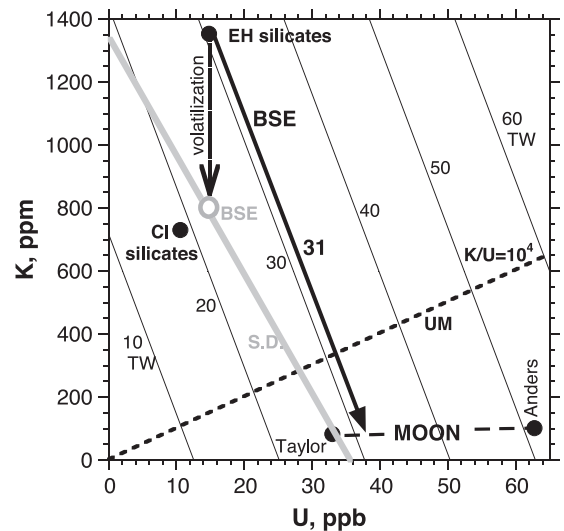


Fig. 7. K vs. U concentrations (weight basis) for planetary materials, exclusive of their metal and sulfide contents. The lunar composition is unaffected by this correction as it lacks a significant core. Compositions shown are the bulk silicate Earth (BSE), Moon, CI and EH chondrites. Light contour lines indicate radioactive powers (as labeled) for a body the size of the silicate Earth assuming  $\text{Th}/\text{U}=3.75$ . Moon compositions are models (Taylor, 1982; Anders, 1977) with uncertainties associated with the variable nature of the lunar surface rocks (Jolliff et al., 2000).  $\text{K}/\text{U}=10^4$  (dotted line) measured for terrestrial rocks (Wasserburg et al., 1964) suggests a range of upper mantle (UM) compositions. Grey line, radioactive contents for a secular delay (s.d.) of 1 Ga, calculated using the tables in Van Schmus (1995). Removal of K preferentially to U and Th by volatilization (dotted line) suggests the BSE composition if cooling is delayed.

The case of delayed secular cooling arising from previous emissions radioactive heat can also be addressed by our method. The decay rates for each of U, Th, and K (Van Schmus, 1995) were used to construct the grey line in Fig. 7, which provides today's rated of 31 TW with a 1 Ga delay. This delay appears to provide an upper limit (Section 2.1). The BSE can lie anywhere on this line.

### 5.1. Possible BSE compositions and K, U, and Th contents for secular cooling rates

If a secular delay exists, neither CI or EH meteorites fall on the line for the BSE. However, the BSE can be derived from EH meteorites by volatilizing K, while the refractories are unchanged, suggesting the composition of 800 ppm K and 15 ppb U for the BSE. The upper mantle (UM) is not constrained in this case, although the compositions of continental crust suggest that the lower mantle (LM) is more enriched in K and less enriched in U or Th than the proposed BSE.

For the case of no secular delay, placing the BSE at a specific point on the line is equivocal, and we discuss the possible cases, made simple to be compatible with scarcity of constraints.

(1) The intersection of the 31 TW isopower line with the K/U ratio of  $10^4$  obtained from terrestrial samples (Wasserburg et al., 1964) provides the concentrations of radioactive elements in the BSE if the UM, transition zone (TZ), and LM all share the same composition (Fig. 7). This possibility is compatible with whole-mantle convection, and with chemical homogeneity on a gross scale.

(2) More likely, the mantle is chemically layered. This case requires layered convection such as the limited penetration style evoked by Silver et al. (1988) or the closed circulation system of Hamilton (2002). Although many mantle convection models lead to whole mantle circulation, all of these unrealistically assume constant thermal conductivity, and assume chemical homogeneity. Incorporating the temperature dependence of  $k$  into a geodynamic model makes layered convection a possibility (Dubuffet et al., 1999). The low thermal conductivity of majorite (Giesting et al., 2003) and the grain-size dependence of radiative transfer (Hofmeister, 2004b, in review) also suggest the possibility of

layered convection. Of course, chemical layering alone could provide layered mantle convection. The linear trend of EH silicates→UM→Moon (Fig. 7) and the likelihood that the outer layers of the Earth are more processed than the inner layers, leads us to place the BSE between EH meteorites and the UM position. The sequence EH silicates→BSE→UM→Moon may result from mixing of the EH type of meteorites and another type (or types) that is high in U and Th with respect to K, for which no sample remains. However, a multi-component model is unnecessary as material closely resembling the EH chondrites could be the source of the Earth–Moon system, but fractionation through volatilization and dust ejection probably occurred during accretion. The popular giant impact model for formation of the Moon by ejection provides an extreme example. Fractionation as the source of the layers in the mantle suggests that EH silicates provide a first-order model of the LM. The LM being wholly comprised of silicate perovskite (i.e. having pyroxene stoichiometry) was considered by Ringwood (1991), and cannot be ruled out on the basis of seismic velocities. This end-member possibility leads to a BSE composition of K=1100 ppm, U=20 ppb, and Th=75 ppb, which is obtained from the masses (LM mass=73% of the BSE).

(3) Another possibility is that the individual mantle layers are off the 31 TW line, but average to place the BSE somewhere on the 31 TW line. This unconstrained scenario is not discussed further.

### 5.2. The core and D'': implications for precursor material

Independent of the above, the average metal–sulfide content of EH chondrites provides both a reasonable mass and composition (80 wt.% Fe, 5 wt.% Ni, and 15 wt.% S) for the Earth's core and D''. Consideration of S in the core can be traced back to Mason's (1966b) analysis of olivine–bronzite chondrites. The nature of light elements in the core is uncertain as seismic and mineral physics data are not sufficient to constrain the composition of this layer (Poirier, 1995), nor of D'', the overlying region. Various arguments and models have been set forth to address this problem. A literal interpretation of enstatite chondrites as

representing the bulk Earth provides more than enough S to explain the density of the core. In fact, so much S is available that  $D''$  could be essentially FeS, given relative densities of Fe and FeS at ambient conditions. The present mass of  $D''$  is smaller than the mass of FeS from EH meteorites, suggesting that core is alloyed with 13 wt.% S, which is within the uncertainty of estimates from geophysical data (e.g. [Boehler, 2000](#)).

Forming the Earth with its massive core from any other class of chondrites requires heterogeneous accretion involving sub-equal amounts of iron meteorites. Not only do these types also have significant troilite ([Mittlefehldt et al., 1998](#)) again leading to S in the core, but most iron meteorites are inferred to have originated as cores of asteroidal bodies. Iron meteorites are better interpreted as differentiated material analogous to Earth's core, rather than Earth's precursor. This comparison reiterates that enstatite chondrites with their high Fe–metal contents are the best available representatives of Earth's precursor material.

No other type of meteorite satisfies the radioactive power, Fe content, and O isotope ratio of the bulk Earth. It is furthermore difficult to address these constraints with a simple mixture, or even a complex mixture, unless enstatite chondrites dominate ([Javoy, 1995](#); [Lodders, 2000](#)). We contend that the ~28,000 meteorite samples in the worldwide collection provide representative precursor material, in the form of EH meteorites, whereas complicated mixing models geared to satisfy unconstrained models of the scarcely sampled mantle rest on shaky ground. It is known that the diverse processes that operate during and after accretion have greatly modified Earth's precursor material, leading to modern layering. The BSE today should thus not exist as an equivalent meteorite. Instead, comparing the Earth to EH meteorites may serve to advance our understanding of its early history.

## 6. Conclusions

The global power is constrained as 30–32 TW ([Table 2](#)) from three approaches utilizing the existing database of oceanic fluxes, which supports earlier

spherical harmonic analyses (e.g. [Lee, 1970](#)). Applying spherical harmonic analyses directly to the data was abandoned in favor of representing the fluxes near the mid-oceanic ridges using the half-space cooling model. This approach assumes boundary conditions inappropriate for the 3-D plates, neglects the temperature dependence of the thermal conductivity and its control on heat flux through Fourier's equation, misrepresents the effect of hydrothermal advection on conductive cooling gradients, and misunderstands the impact that infinite heat flux at ages of  $t=0$  (all ridge axes over all time) and the chosen value of  $k$  have in determining the oceanic mean using the half-space cooling model. Rationalization of the large discrepancy between model and measurements as arising from lateral heat flow due to hydrothermal circulation is not only inconsistent with the derivation of the HSC model, but requires Rayleigh numbers far in excess of published values. The original proposal of [Lister \(1972\)](#) considered hydrothermal circulation to operate locally, and subsequent analyses ([Elder, 1981](#)) inferred that these systems are limited to within ~10 km of the ridge.

Use of the HSC model has led to a perceived global power that is disparate with radioactive power generated by a CI model. For the most part, the CI model, or mixing models, have been invoked as providing the bulk chemistry of the Earth, but because none of these can account for the 44 TW of [Pollack et al. \(1993\)](#), the difference has been rationalized as additional heat from delayed secular cooling and other sources. Recent geodynamics studies ([Van den Berg and Yuen, 2002](#); [Van den Berg et al., 2002](#)) provide an upper limit on the delays of ~1 billion years, which is too short for delayed secular cooling to provide a significant source of heat today, and in particular to account for the discrepancy between the surface power of 31 TW and a CI model. The EH model of the bulk silicate Earth discussed here can account for the radioactive power, as well as the other known markers, the Fe content and oxygen isotopes. The model is necessarily vague, to allow for the poorly constrained chemistry of the lower mantle, and the possible presence of a small secular delay, but provides end-member compositions for K, U, and Th contents.

## Acknowledgments

The input of D.L. Anderson, B. Fegley, W.B. Hamilton and K. Lodders is gratefully acknowledged. Support was provided by EAR-00125883.

## References

- Abbott, D., Burgess, L., Longhi, J., 1994. An empirical thermal history of the Earth's upper mantle. *J. Geophys. Res.* 99, 13835–13850.
- Anders, E., 1977. Chemical compositions of the moon, Earth and eucrite parent body. *Philos. Trans. R. Soc. Lond., A* 285, 23–40.
- Anderson, D.L., 1988. A model to explain the various paradoxes associated with mantle noble gas geochemistry. *Proc. Natl. Acad. Sci.* 95, 9067–9092.
- Anderson, O.L., 1988. The Grüneisen parameter for iron at outer core conditions and the resulting conductive heat and power in the core. *Phys. Earth Planet. Inter.* 109, 179–197.
- Anderson, O.L., 2002. The power balance at the core–mantle boundary. *Phys. Earth Planet. Inter.* 131, 1–17.
- Boehler, R., 2000. High pressure experiments and the phase diagram of lower mantle and core materials. *Rev. Geophys.* 38, 221–245.
- Brearily, A.J., Jones, R.H., 1998. Chondritic meteorites. *Rev. Miner.* 36, 3-1–3-398.
- Breuer, D., Spohn, T., 1993. Cooling of the Earth, Urey ratios, and the problem of potassium in the core. *Geophys. Res. Lett.* 20, 1655–1658.
- Buettner, R., Zimanowski, B., Blumm, J., Hagermann, L., 1998. Thermal conductivity of a volcanic rock material (olivine–melilitite) in the temperature range between 298 and 1470 K. *J. Volcanol. Geotherm. Res.* 80, 293–302.
- Buffett, B.A., 2002. Estimates of heat flow in the deep mantle based on the power requirements for the geodynamo. *Geophys. Res. Lett.* 29 (12), 7-1–7-4.
- Burke, K.C., Kidd, W., Turcotte, D., Dewey, J., Mouginiis-Mark, P., Parmentier, E., Sengor, A.M., Tapponnier, P., 1981. Tectonics of basaltic volcanism. In: *Basaltic Volcanism Study Project* (Ed.), *Basaltic Volcanism of the Terrestrial Planets*. Pergamon Press Inc., New York, pp. 803–898.
- Carslaw, H.S., Jaeger, J.C., 1959. *Conduction of Heat in Solids*. Clarendon Press, Oxford.
- Chapman, D.S., Pollack, H.N., 1980. Global heat flow: Spherical harmonic representation. *EOS Trans.-Am. Geophys. Union* 61, 383.
- Chapman, D.S., Rybach, L., 1985. Heat flow anomalies and their interpretation. *J. Geodyn.* 4, 30–37.
- Clayton, R.N., 1993. Oxygen isotopes in meteorites. *Annu. Rev. Earth Planet. Sci.* 21, 115–149.
- Criss, R.E., Champion, D.E., 1991. Oxygen isotope study of the fossil hydrothermal system in the Comstock Lode mining district, Nevada. *Spec. Publ.-Geochem. Soc.* 3, 437–447.
- Criss, R.E., Hofmeister, A.M., 1991. Application of fluid dynamics principles in tilted permeable media to terrestrial hydrothermal systems. *Geophys. Res. Lett.* 18, 199–202.
- Criss, R.E., Taylor, H.P., 1986. Meteoric–hydrothermal systems. *Rev. Miner.* 16, 373–424.
- Drake, M.J., Righter, K., 2002. Determining the composition of the Earth. *Nature* 416, 39–44.
- Dubuffet, F., Yuen, D.A., Rabinowicz, M., 1999. Effects of a realistic mantle thermal conductivity on the patterns of 3-D convection. *Earth Planet. Sci. Lett.* 171, 401–409.
- Dubuffet, F., Yuen, D.A., Rainey, E.S.G., 2002. Controlling thermal chaos in the mantle by positive feedback from radiative thermal conductivity. *Nonlinear Process. Geophys.* 9, 1–13.
- Elder, J., 1981. *Geothermal Systems*. Academic Press, London, p. 182 ff.
- Elderfield, H., Schultz, A., 1996. Mid-Ocean ridge hydrothermal fluxes and the chemical composition of the ocean. *Annu. Rev. Earth Planet. Sci.* 24, 191–224.
- Faure, G., 1986. *Isotope Geology*. John Wiley and Sons, New York.
- Galer, S.J.G., Mezger, K., 1998. Metamorphism, denudation and sea level in the Archean and cooling of the Earth. *Precambrian Res.* 92, 389–412.
- Gasparik, T., 2000. Evidence for the transition zone origin of some [Mg,Fe]O inclusions in diamonds. *Earth Planet. Sci. Lett.* 183, 1–5.
- Gessmann, C.K., Wood, B.J., 2002. Potassium in the Earth's core? *Earth Planet. Sci. Lett.* 200, 63–78.
- Giesting, P.A., Hofmeister, A.M., Wopenka, B., Gwanmesia, G.D., Jolliff, B.L., 2003. Thermal conductivity and thermodynamic properties of majorite: implications for the transition zone. *Earth Planet. Sci. Lett.* 218, 45–56.
- Goldstein, S.J., Jacobsen, S.B., 1987. The Nd and Sr isotopic systematics of river-water dissolved material: implications for the sources of Nd and Sr in seawater. *Chem. Geol.* 66, 244–272.
- Gosnold, W.D., Panda, B., 2002. Interim compilation of the International Heat Flow Commission (<http://www.heatflow.org>). Accessed September 22.
- Gregory, R.T., 1991. Oxygen isotope history of seawater revisited: timescales for boundary even changes in the oxygen isotope composition of seawater. *Spec. Publ.-Geochem. Soc.* 3, 65–76.
- Gregory, R.T., Taylor, H.P., 1981. An oxygen isotope profile in a section of Cretaceous oceanic crust, Samail ophiolite, Oman: Evidence for  $\delta^{18}\text{O}$ -buffering of the oceans by deep (>5 km) seawater–hydrothermal circulation at mid-ocean ridges. *J. Geophys. Res.* 86, 2737–2755.
- Gubbins, D., 1977. Energetics of the Earth's core. *J. Geophys.* 43, 453–464.
- Hamilton, W.B., 2002. The closed upper-mantle circulation of plate tectonics. In: Stein, S., Freymueller, J.T. (Eds.), *Plate Boundary Zones, Geodynamics Series*, vol. 30. American Geophysical Union, Washington, DC, pp. 359–410.
- Hofmeister, A.M., 1999. Mantle values of thermal conductivity and the geotherm from photon lifetimes. *Science* 283, 1699–1706.
- Hofmeister, A.M., 2004a. Enhancement of radiative transfer in the mantle by OH<sup>-</sup> in minerals. *Phys. Earth Planet. Inter.* 146, 483–495.

- Hofmeister, A.M., 2004b. Thermal conductivity and thermodynamic properties from infrared spectroscopy. In: King, P., Ramsey, M., Swayze, G. (Eds.), *Infrared Spectroscopy in Geochemistry, Exploration Geochemistry, and Remote Sensing*, Mineralogical Association of Canada, Short Course, vol. 33, pp. 135–154.
- Hofmeister, A.M., in review. The dependence of diffusive radiative transfer on grain-size, temperature, and pressure: implications for mantle processes. *Pure and Appl. Geophysics*.
- Hofmeister, A.M., Mao, H.K., 2003. Pressure derivatives of shear and bulk moduli from the thermal Grüneisen parameter and volume–pressure data. *Geochim. Cosmochim. Acta* 67, 1207–1227.
- Horai, K., 1971. Thermal conductivity of rock-forming minerals. *J. Geophys. Res.* 76, 1278–1308.
- Horai, K., Simmons, G., 1969. Spherical harmonic analysis of terrestrial heat flow. *Earth Planet. Sci. Lett.* 6, 386–394.
- Javoy, M., 1995. The integral enstatite chondrite model of the Earth. *Geophys. Res. Lett.* 22, 2219–2222.
- Jessop, A.M., Hobart, M.A., Sclater, J.G., 1976. The world heat low data collection—1975. *Geotherm. Ser.* 5, 125 pp.
- Johnson, H.P., Pruis, M.J., 2003. Fluxes of fluid and heat from the oceanic crustal reservoir. *Earth Planet. Sci. Lett.* 216, 565–574.
- Jolliff, B.L., Gillis, J.J., Haskin, L.A., 2000. Thorium mass balance for the Moon from lunar prospector and sample data: implications for thermal evolution. *Lunar Planet. Sci. Conf.* 31, 1763.
- Kanamori, H., Fujii, N., Mizutani, H., 1968. Thermal diffusivity measurement of rock-forming minerals from 300 to 1100 K. *J. Geophys. Res.* 73, 595–603.
- Labrosse, S., 2003. Thermal and magnetic evolution of the Earth's core. *Phys. Earth Planet. Inter.* 140, 127–143.
- Lee, W.H.K., 1963. Heat flow data analysis. *Rev. Geophys.* 1, 449–479.
- Lee, W.H.K., 1970. On the global variations of terrestrial heat-flow. *Phys. Earth Planet. Inter.* 2, 332–341.
- Lee, W.H.K., Uyeda, S., 1965. Review of heat flow data. In: Lee, W.H.K. (Ed.), *Terrestrial Heat-Flow*, *Geophys. Monogr. Ser.* vol. 8. AGU, Washington, DC, pp. 87–100.
- Liebfried, G., Schlömann, E., 1954. Warmleitend in elektrische isolierenden Kristallen. *Nachr. Ges. Wiss. GoÉtt., Math.-Phys. Kl.*, 71–93.
- Lister, C.R.B., 1972. On the thermal balance of a mid-ocean ridge. *Geophys. J. R. Astron. Soc.* 26, 515–535.
- Lodders, K., 1995. Alkali elements in the Earth's core: evidence from enstatite meteorites. *Meteoritics* 30, 93–101.
- Lodders, K., 2000. An oxygen isotope mixing model for the accretion and composition of rocky planets. *Space Sci. Rev.* 92, 341–354.
- Lodders, K., Fegley Jr., B.J., 1998. *The Planetary Scientist's Companion*. Oxford University Press, Oxford.
- MacDonald, G.J.F., 1959. Chondrites and the chemical composition of the Earth. In: Abelson, P.H. (Ed.), *Researches in Geochemistry*. John Wiley & Sons, New York, pp. 476–494.
- Mason, B., 1966a. Composition of the Earth. *Nature* 211, 616–618.
- Mason, B., 1966b. The enstatite chondrites. *Geochim. Cosmochim. Acta* 30, 23–39.
- McKenzie, D., Richter, F.M., 1981. Parameterized thermal convection in a layered region and the thermal history of the Earth. *J. Geophys. Res.* 86, 11667–11680.
- Mittlefehldt, D.W., McCoy, T.J., Goodrich, C.A., Kracher, A., 1998. Non-chondritic meteorites from asteroidal bodies. *Rev. Miner.* 36, 4-1–4-195.
- Norton, D., Knight, J., 1977. Transport phenomena in hydrothermal systems: Cooling plutons. *Am. J. Sci.* 277, 937–981.
- Norton, D., Taylor Jr., H.P., 1979. Quantitative simulation of the hydrothermal systems of crystallizing magmas on the basis of transport theory and oxygen isotope data: an analysis of the Skaergaard intrusion. *J. Petrol.* 20, 421–486.
- Parsons, B., Sclater, J.G., 1977. An analysis of the variation of ocean floor bathymetry and heat flow with age. *J. Geophys. Res.* 82, 803–827.
- Poirier, J.P., 1995. Light elements in the Earth's core: a critical review. *Phys. Earth Planet. Inter.* 85, 319–337.
- Pollack, H.N., Hurter, S.J., Johnson, J.R., 1993. Heat flow from the Earth's interior: analysis of the global data set. *Rev. Geophys.* 31, 267–280.
- Rama Murthy, V., van Westrenen, W., Fei, Y., 2003. Experimental evidence that potassium is a substantial radioactive heat source in planetary cores. *Nature* 423, 163–165.
- Ringwood, A.E., 1991. Phase transformation and their bearing on the constitution and dynamics of the mantle. *Geochim. Cosmochim. Acta* 55, 2110–2803.
- Roberts, P.H., Jones, C.A., Calderwood, A.R., 2003. Energy fluxes and Ohmic dissipation in the Earth's core. In: Jones, C.A., Soward, A.M., Zhang, K. (Eds.), *Earth's Core and Lower Mantle*. Taylor, London.
- Rubin, A., 1997. Mineralogy of meteorite groups. *Meteorit. Planet. Sci.* 32, 231–247.
- Schatz, J.F., Simmons, G., 1972. Thermal conductivity of Earth materials at high temperature. *J. Geophys. Res.* 77, 6966–6983.
- Silver, P.G., Carlson, R.W., Olson, P., 1988. Deep slabs, geochemical heterogeneity and large-scale structure of mantle convection. *Annu. Rev. Earth Planet. Sci.* 16, 477–541.
- Singleton, M.J., Criss, R.E., 2004. Symmetry of flow in the Comstock Lode hydrothermal system: evidence for longitudinal convective rolls in geologic systems. *J. Geophys. Res.* 109 (B03205), 15 pp.
- Sinogeikin, S.V., Bass, J.D., 2002. Elasticity of majorite and a majorite–pyrope solid solution to high pressure: implications for the transition zone. *Geophys. Res. Lett.* 29 (paper, 4 pp.).
- Slack, G., 1962. Thermal conductivity of MgO, Al<sub>2</sub>O<sub>3</sub>, MgAl<sub>2</sub>O<sub>4</sub>, and Fe<sub>3</sub>O<sub>4</sub> crystals from 3 to 300K. *Phys. Rev.* 126, 427–441.
- Sleep, N.H., Wolery, T.J., 1978. Egress of hot water from midocean ridge hydrothermal systems: some thermal constraints. *J. Geophys. Res.* 83, 5913–5922.
- Solomatov, V.S., 2001. Grain-size dependent viscosity convection and the thermal evolution of the Earth. *Earth Planet. Sci. Lett.* 191, 203–212.
- Stacey, F.D., 1969. *Physics of the Earth*. John Wiley and Sons, New York.
- Stacey, F.D., Anderson, O.L., 2001. Electrical and thermal conductivities of Fe–Ni–Si alloy under core conditions. *Phys. Earth Planet. Inter.* 124, 153–162.

- Stein, C.A., Stein, S.A., 1992. A model for the global variation in oceanic depth and heat flow with lithospheric age. *Nature* 359, 123–128.
- Sundqvist, B., 1981. Thermal conductivity and Lorentz number of nickel under pressure. *Solid State Commun.* 37, 289–291.
- Sundqvist, B., 1982. In: Backman, C.M., Johannison, T., Tegner, L. (Eds.), *High Pressure in Research and Industry*, pp. 432–433.
- Taylor, S.R., 1982. Lunar and terrestrial crusts: a contrast in origin and evolution. *Phys. Earth Planet. Inter.* 29, 233–241.
- Tozer, D.C., 1979. Heat transfer and convection currents. *Philos. Trans. R. Soc. Lond. Ser. A: Math. Phys. Sci.* 301, 381–399.
- Triton, D.J., 1988. *Physical Fluid Dynamics*. Clarendon Press, Oxford.
- U.S.G.S. (United States Geological Survey) ([pubs.usgs.gov/publications/text/Pangaea/html](http://pubs.usgs.gov/publications/text/Pangaea/html)). Accessed September 22, 2002.
- Van den Berg, A.P., Yuen, D., 2002. Delayed cooling of the Earth's mantle due to variable thermal conductivity and the formation of a low conductivity zone. *Earth Planet. Sci. Lett.* 199, 403–413.
- Van den Berg, A.P., Yuen, D.A., Steinbach, V.C., 2001. The effects of variable thermal conductivity on mantle heat-transfer. *Geophys. Res. Lett.* 28, 875–878.
- Van den Berg, A.P., Yuen, D.A., Allwardt, J.R., 2002. Non-linear effects from variable thermal conductivity and mantle internal heating: Implications for massive melting and secular cooling of the mantle. *Phys. Earth Planet. Inter.* 129, 359–375.
- Van Schmus, W.R., 1995. Natural radioactivity of the crust and mantle. In: Ahrens, T.J. (Ed.), *Global Earth Physics*. American Geophysical Union, Washington, DC, pp. 283–291.
- Wasserburg, G.J., MacDonald, G.J.F., Hoyle, F., Fowler, W.F., 1964. Relative contributions of uranium, thorium, and potassium to heat production in the Earth. *Science* 143, 465–467.